Recurrent Convolutional Neural Network-Based Assessment of Power System Transient Stability and Short-Term Voltage Stability

Tapia, Estefania Alexandra ; Colomé, Delia Graciela ; Rueda, José L.

DOI
10.3390/en15239240

Publication date
2022

Document Version
Final published version

Published in
Energies

energies

MDPI

Article

Recurrent Convolutional Neural Network-Based Assessment of Power System Transient Stability and Short-Term Voltage Stability

Estefania Alexandra Tapia [1], Delia Graciela Colomé [1] and José Luis Rueda Torres [2,*]

[1] Electrical Energy Institute, Universidad Nacional de San Juan—CONICET, San Juan 5400, Argentina
[2] Department of Electrical Sustainable Energy, Delft University of Technology (TU Delft), 2628 CN, The Netherlands
* Correspondence: j.l.ruedatorres@tudelft.nl

Abstract: Transient stability (TS) and short-term voltage stability (STVS) assessment are of fundamental importance for the operation security of power systems. Both phenomena can be mutually influenced in weak power systems due to the proliferation of power electronic interface devices and the phase-out of conventional heavy machines (e.g., thermal power plants). There is little research on the assessment of both types of stability together, despite the fact that they develop over the same short-term period, and that they can have a major influence on the overall transient performance driven by large electrical disturbances (e.g., short circuits). This work addresses this open research challenge by proposing a methodology for the joint assessment of TS and STVS. The methodology aims at estimating the resulting short-term stability state (STSS) in stable, or unstable conditions, following critical events, such as the synchronism loss of synchronous generators (SG) or the stalling of induction motors (IM). The estimations capture the mechanisms responsible for the degradations of TS and STVS, respectively. The paper overviews the off-line design of the data-driven STSS classification methodology, which supports the design and training of a hybrid deep neural network RCNN (recurrent convolutional neural network). The RCNN can automatically capture spatial and temporal features from the power system through a time series of selected physical variables, which results in a high estimation degree for STSS in real-time applications. The methodology is tested on the New England 39-bus system, where the results demonstrate the superiority of the proposed methodology over other traditional and deep learning-based methodologies. For reference purposes, the numerical tests also illustrate the classification performance in special situations, when the training is performed by exclusively using measurements from generation and motor load buses, which constitute locations where the investigated stability can be observed.

Keywords: transient stability (TS); short-term voltage stability (STVS); recurrent convolutional neural networks (RCNN); convolutional neural network (CNN); long short-term memory network (LSTM); real-time prediction

Citation: Tapia, E.A.; Colomé, D.G.; Rueda Torres, J.L. Recurrent Convolutional Neural Network-Based Assessment of Power System Transient Stability and Short-Term Voltage Stability. *Energies* **2022**, *15*, 9240. https://doi.org/10.3390/en15239240

Academic Editor: Abu-Siada Ahmed

Received: 3 November 2022
Accepted: 25 November 2022
Published: 6 December 2022

1. Introduction

Transient stability (TS) and short-term voltage stability (STVS) represent a major concern in weak power systems' operation and planning [1,2], as major collapses have been attributed to these types of stability [3]. Since TS and STVS develop over a short-term period, these two phenomena have an important influence on the overall transient response after a large disturbance, i.e., both phenomena can contribute to instability development in the same time window [1]. However, TS and STVS are generally studied separately because their instability factors are usually considered to have a different nature, i.e., TS is associated with synchronous generators' (SGs') dynamics through their synchronism loss, whereas STVS is associated with the loads' dynamics through induction motor (IMs) stalling. As TS and STVS have different instability mechanisms, the emergency control actions for

their mitigation also differ. In this sense, it is of fundamental importance to consider both dynamics, generation and load, to more accurately assess the system's short-term stability state (SST) and determine the dominant driving force of instability. Such an assessment is needed for confidently defining emergency control actions to prevent propagation of the resulting system instability.

Nowadays, with the fast development of artificial intelligence (AI) techniques and the use of PMU measurements, different data-driven machine learning methods have proven to be capable of the predictive assessment of TS and STVS. For example, studies aimed at assessing TS have used support vector machines (SVM) [4,5], decision trees [6], K-nearest neighbors [7], and extreme learning machines (ELM) [8,9]. Likewise, researchers that have assessed STVS have also used SVM algorithms [10], ELMs based on artificial neural networks (ANN) [10], and random forests [11]. However, since the learning algorithms' performance is highly dependent on the input data representation, careful engineering and considerable field experience are of great importance, so that the internal representation design can allow the algorithm to make correct decisions [12].

Deep learning (DL) solves the limitations of traditional learning methods by allowing a machine to be fed raw data with the help of more hidden layers and automatically discover features needed for classification without relying on experience. Due to the improvement in computational performance and data capacity, various methodologies for assessing system stability based on deep learning have emerged in recent years. For example, methodologies that assess TS have used deep neural networks, such as stacked autoencoders (SAE) applied in two stages (initialization and classification) [13], long- and short-term memory (LSTM) networks [14] and gated recurrent units (GRU) [15] in the learning of time series correlations, and convolutional neural networks (CNN) due to their ability to extract spatial features and fast training convergence [16,17]. Likewise, researchers that have studied STVS have used DL techniques, such as recurrent neural networks (RNN) based on the LSTM model [18], due to their ability to extract temporal features, and graphical neural networks (GNN) [19] for their ability to extract topological information from the network that has undergone adaptation to topological changes. Additionally, hybrid models have also been proposed, such as [20], that use graphical convolutional networks (GCN) together with LSTM and form the model called the recurrent graph convolutional network (RGCN). RGCNs can capture spatial-temporal features and extract topological information from the network; this information is used to classify the TS state and determine critical generators that lead to instability development. The RGCN model has also been used in the study of STVS by [21], where they use this model to predict and locate unstable buses following a disturbance occurrence.

Although the different methodologies based on AI models that study TS and STVS have highly reliable, robust, or scalable characteristics, none of them jointly consider the generation dynamics and the load dynamics. That is, studies focused on TS assume that only generation dynamics are presented since they model the load only with static characteristics, while studies focused on STVS assume that only load dynamics are presented since the model generation simply involves ideal voltage sources [22]. In other words, the investigations start from the assumption that the dominant mechanism of instability is already known through the limited modeling of the system's dynamics.

Recently, a few works have considered the joint dynamics of generation and loads and tried to determine the main driving force of instability. In [23], they use the stable-state Thevenin equivalent circuit to determine the unstable equilibrium point (UEP) and then compare this point with IM slips and GS rotor angles; however, this proposal does not guarantee reliable results. In [22], based on a double generation one-load (DGOL) model, they establish a two-dimensional index that quantifies the stalling margin of IM and the angle deviation margin of SG; however, the precision of this methodology depends on an extensive adjustment process of the DGOL model with parameter determination for certain contingency cases. In [24], for a few faults, the authors compare the rotor angle trajectories of SG with the voltage buses of IM, where the greater number of components (IM or SG) that lose stability the earliest after the failure corresponds to the dominant factor

of instability; however, this is a criterion that lacks reliability. More recent research [25] calculates the UEP and analyzes the trajectories of the SG rotor angles and the IM speed to identify the instability mechanism; this is information that is used to train decision trees, as a traditional ML algorithm, and in real-time, the STSS can be determined as stable or unstable due to STVS, or unstable due to TS. The stability status classification results of this methodology, together with the other studies mentioned, were verified by shedding motor loads or tripping SG, where, depending on the disconnected component, the corresponding type of instability was mitigated. The work proposed in [25] is the only study that focuses on its application in real-time based on ML models; nevertheless, the selected model requires complex mathematical calculations to obtain the necessary features, and the decision trees can make correct decisions.

In a departure from the above-discussed state-of-the-art, the present work proposes a methodology for the joint assessment of TS and STVS, which predicts in real-time the STSS (stable or unstable performance due to STVS, or unstable performance due to TS). The methodology is based on a combination of DL algorithms that are able to capture spatial and temporal features automatically, with a high potential regarding applicability and performance, particularities that are demonstrated by CNN and LSTM models, which form the model named the recurrent convolutional neural network (RCNN). The methodology classifies the STSS offline with a different approach to the traditional methods; that is, instead of carrying out the development of complex algorithms with calculations that require high accuracy and computational effort, the results of the component disconnection responsible for the stability loss, together with the monitoring of a representative variable, are used.

The main contributions of this work are follows:

- A novel real-time predictive assessment methodology of TS and STVS states under a severe contingency scenario is developed. The methodology is based on the DL model named RCNN, which combines CNN and LSTM models to capture spatial and temporal features from the power system variables.
- The predictive assessment model can be implemented in real-time, allowing lead emergency control actions and preventing the spread of instability in the system.
- The STSS offline classification methodology is performed based on monitoring a representative variable from the system and the application of emergency control actions directed at the possible instability mechanism. The approach does not require high-accuracy calculations or high computational effort.
- An RCNN deep learning model with a high degree of performance that requires, as input data, electrical variables that are measurable by PMU devices on all buses or only on strategic buses (generation and motor loads) over a short time period. The model presents rapid classification results before the development of instability, allowing emergency control actions to be implemented.

The remainder of this paper is organized as follows. Section 2 presents a brief overview of the background of the study and the causes of TS and STVS loss. Section 3 presents the proposed RCNN model. Section 4 gives a detailed description of the model training process and its real-time application. Section 5 presents the results of the methodology implemented on the New England 39-bus test system. Finally, Section 6 presents the conclusions of this work.

2. Short-Term Stability State

In the framework of short-term analysis, transient stability (TS) and voltage stability (STVS) have drawn increasing concerns for the electric industry sector. Historically, transient instability has been the dominant factor of many collapses in transmission systems. Nevertheless, due to the increase in loads with dynamic fast-acting characteristics, such as induction motors, STVS has also become a determining factor for the short-term stability condition and, therefore, a greater concern [1,3].

2.1. Transient Stability (TS)

TS refers to a system's ability to remain in synchronism following a severe disturbance. This depends on every SG's ability to maintain or restore the balance between mechanical and electromagnetic torques. Transitory instability is reflected through the rotor angle increase in some SGs, leading to the loss of their synchronism [26]. Generally, in these situations, the SG tripping due to the action of out-of-step relays as an emergency control action can be executed to maintain stability and reduce losses resulting from faults [27].

2.2. Short-Term Voltage Stability (STVS)

Short-term voltage stability refers to the attempt of load dynamics to restore power consumption beyond the capability of the combined transmission and generation system [28]. That is, when a severe fault occurs, dynamics loads, such as IMs, begin to stall and draw excessive reactive power from the grid. If the reactive power resources are not able to deliver the instantaneous power required by the load, mechanical and electromagnetic torque curves cannot be intercepted, the voltage cannot be recovered and finally, the system may culminate in an unstable condition [29]. In this case, the IM load shedding, as an emergency control action, can avoid the instability propagation [30].

The STVS problem can be reflected through the following three phenomena shown in Figure 1: sustained low voltage, fault-induced delayed voltage recovery (FIDVR), and rapid voltage collapse [3]. Among these STVS phenomena, rapid voltage collapse is considered the most serious unstable condition for the system, and it is also frequently associated with TS problems. Therefore, in this work, only rapid voltage collapse response is considered as an unstable voltage condition in the short term.

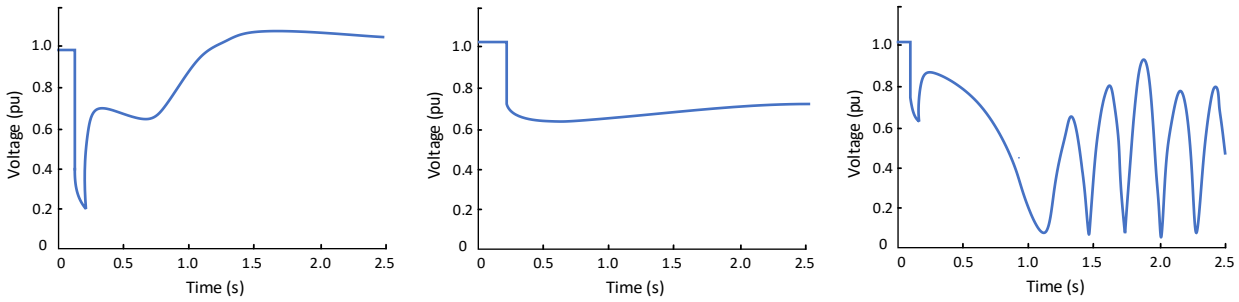

Figure 1. Short-term voltage stability phenomena: (**a**) FIDVR; (**b**) sustained low voltage; (**c**) rapid voltage collapse.

3. Recurrent Convolutional Neural Network

The DL hybrid model, named the recurrent convolutional neural network (RCNN), is composed of CNN and LSTM models and is able to establish a relationship between the power system measurement data (during the fault and a very short time after the clearance) and the short-term stability state (STSS). Figure 2 shows the overall framework of the RCNN.

As can be observed in Figure 2, first of all, the measurement data are processed in a grid-like topology (analogous to images). Then, this information is entered into the RCNN model, where automatic extraction of spatial and temporal features is performed for STSS classification.

The RCNN model, as Figure 2 indicates, consists of the following four cascaded modules: convolutional layers (CNN), fully connected (FC) layers, long short-term memory (LSTM) layers, and the classifier. The CNN and LSTM are hierarchical modules, while the fully connected layers and the classifier are singular modules. On the one hand, the hierarchical modules represent the RCNN fundamental basis, since they deal with spatial and temporal feature extraction; in addition, by presenting a stacked structure, they also contain pooling, dropout, normalization, and FC layers. On the other hand, the singular modules that correspond to the fully connected layers and the classifier are in charge of

establishing a link with the extracted features and detecting the STSS, respectively. Details of these modules are presented below.

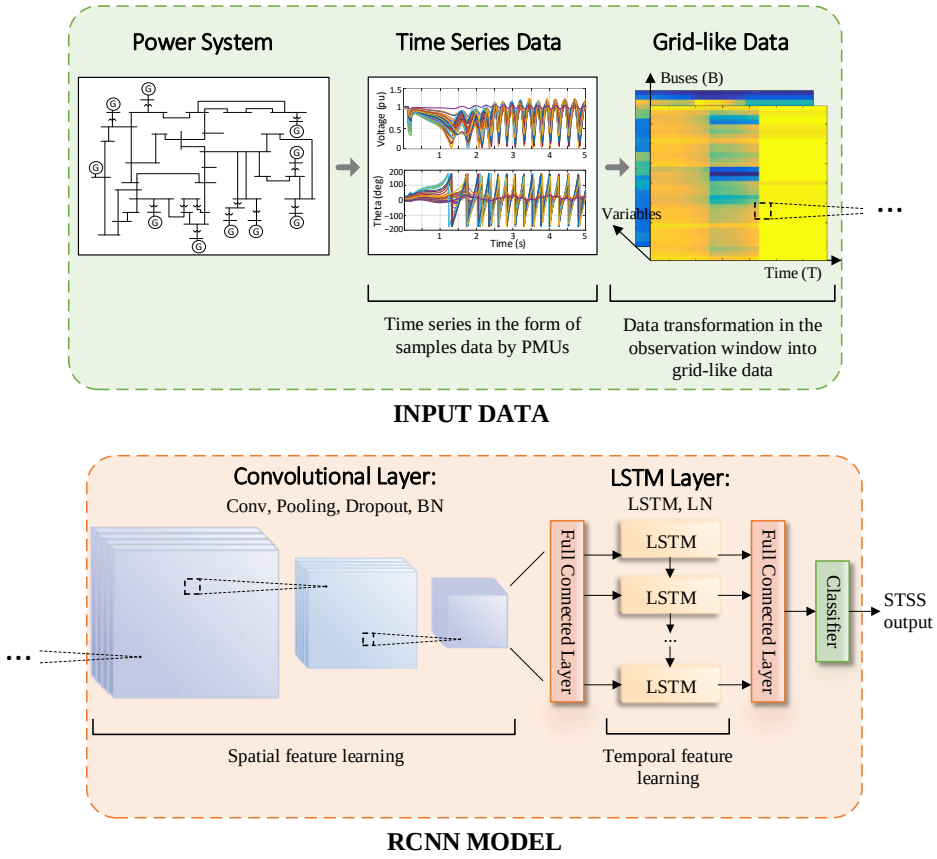

Figure 2. Overall framework of RCNN model.

3.1. Convolutional Neural Network Layer

Convolutional neural networks (CNN) are based on the mapping of spatial features by convolution operations in multidimensional data [31]. The feature mapping of CNN contains k filters that are spatially repartitioned into different channels. The convolutional layer y_i is calculated as $y_i = f_a\left(\sum_i k_{ij} x_{ij}\right)$, where x_i, k_i, and y_i denote the feature input, the convolution kernel, and the hidden layer of the ith iteration, respectively, while f_a represents the activation function [32].

CNNs analyze the hidden patterns using pooling layers for scaling, shared weights for memory reduction, filters for detecting correlations by convolution operations, and also dropout for reducing overfitting that is often shown by networks [32].

3.2. Long-Short Term Memory Layer

As one of the most popular variants of recurrent neural networks (RNN), LSTM is known for its excellent ability to extract temporal features from sequential input data [33]. In addition, it has the ability to overcome the problem of RNN vanishing gradients, that is, when the backward gradient becomes very small, and the previous layers cannot change the settings, which causes the neural network to stop learning [34].

The LSTM structure, as shown in Figure 3, comprises three memory gates called input, forget, and output gates. These are responsible for selecting and rejecting the information that passes through the network. x_t, c_t, h_t and σ represent the input vectors, the memory unit, the hidden states, and the activation function, respectively [34].

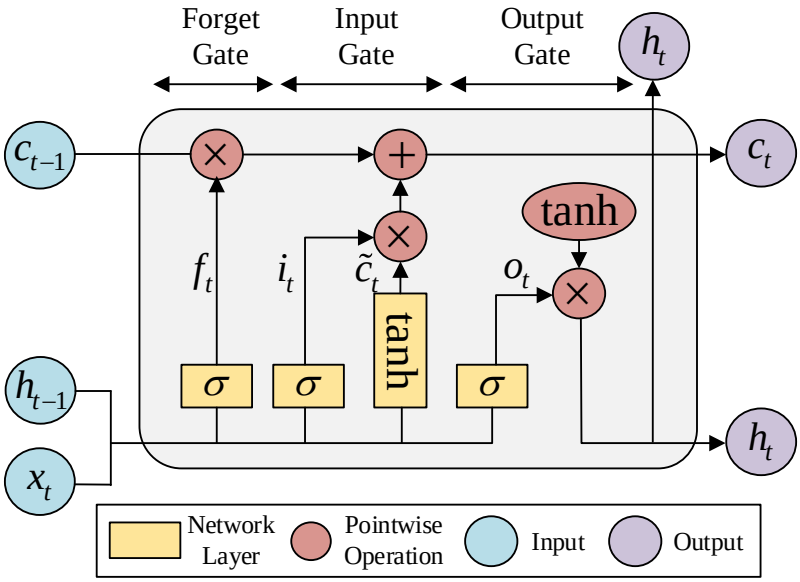

Figure 3. Representation of LSTM cell.

3.3. Fully Connected Layer

The output of an FC layer corresponds to the linear transformation of the inputs [35]. On the one hand, the RCNN's FC layers allow the spatial features extracted from the CNN module to enter into the LSTM module and, on the other hand, they enable the temporal features captured from the LSTM module to predict the STSS results through the classifier.

3.4. Classifier

The STSS prediction can be expressed as a multiclass classification problem in stable and unstable systems due to SG out-of-synchronism (TS), or unstable systems due to IM stalling (STVS), with each class being mutually exclusive. The activation function used is softmax, which gives the confidence $\widetilde{c}_i$ for the category i as follows:

$$\widetilde{c}_i = \frac{e^{z_i}}{\sum_i e^{z_i}} (i = 1,\ 2,\ 3) \tag{1}$$

where $\widetilde{c}_1 + \widetilde{c}_2 + \widetilde{c}_3 = 1$; and z_i are the values of each class. Therefore, the STSS was predicted as detailed in Table 1.

Table 1. Multiclass classifier results of STSS.

STSS	Softmax Result	Label
Stable	$\widetilde{c}_1 > 0.5$	(1, 0, 0)
Unstable due to TS	$\widetilde{c}_2 > 0.5$	(0, 1, 0)
Unstable due to STVS	$\widetilde{c}_3 > 0.5$	(0, 0, 1)

4. Proposed RCNN-Based Methodology

The methodology that follows the RCNN model implementation is developed in three stages, which are shown in Figure 4.

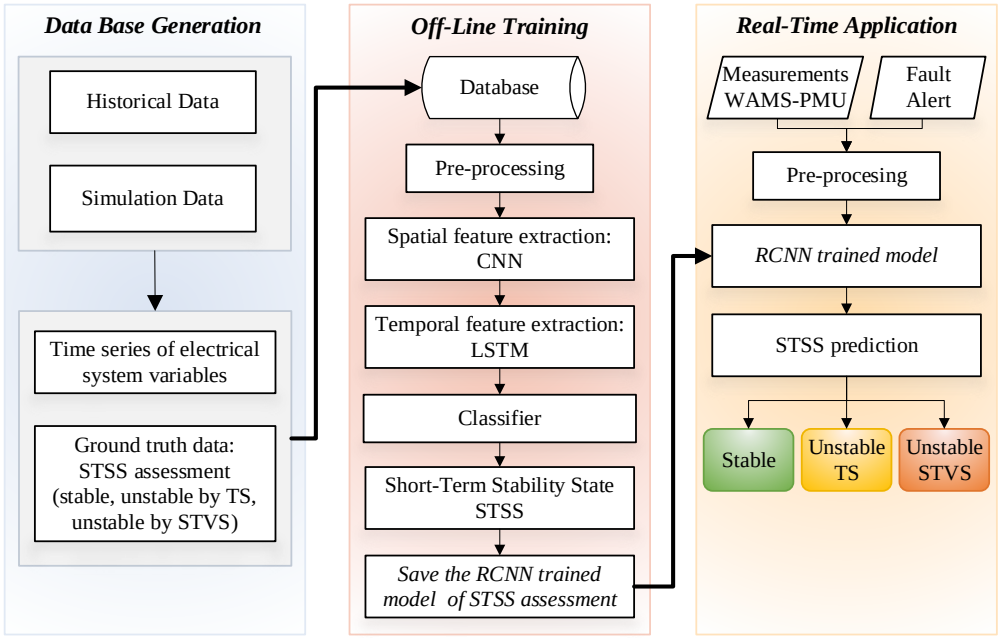

Figure 4. Flowchart of the proposed RCNN-based methodology and its real-time application.

4.1. Database Generation

The RCNN model training requires a database that can be generated from historical data or from time-domain simulations (TDS) if the historical data are insufficient. The database comprises (a) a time series of electrical system variables; and (b) sample labeling, that is, the STSS of each contingency case. Each aspect comprises the database that is detailed below.

4.1.1. Time Series of Electrical System Variables as RCNN Input Data

The RCNN input data correspond to the time series of the electrical system variables that allow the STSS assessment task to be developed with great precision and within a small time window. In other words, it is thought that the selected variables effectively reflect the problem to be assessed and can be measured using PMU devices for the subsequent real-time model application.

On the one hand, the TS assessment is usually performed by monitoring the variables that correspond to the rotor angles or angular speed of the SG; however, different studies, such as [36,37], indicate that the voltage angle can reflect the SG status, has a much faster response than the other variables, and possesses the advantage of being measured directly by PMU devices. On the other hand, the STVS assessment is generally conducted using the variable that corresponds to the voltage magnitude (U), since it directly reflects the voltage state and can also be measured directly by PMU devices. Therefore, this work selects the voltage phasors (U, θ) as input data for the RCNN model.

In the first instance, the voltage phasors measured correspond to the buses of the entire system within a very short time window from the fault occurrence. In Section 5.4.2, the RCNN model performance is analyzed, where the training data only contains data of generation and motor load buses, locations that directly reflect the stability problems under study.

4.1.2. Offline STSS Labeling

As mentioned, the STSS assessment, in the face of a severe disturbance, is used to analyze whether the system is stable or unstable due to TS, or unstable due to STVS. In this sense, a methodology that classifies the offline STSS is implemented, which is based on monitoring a representative variable that indicates when the system is stable or unstable,

and on applying emergency control actions aimed at the possible instability mechanism. Each aspect of the methodological basis for STSS classification is discussed below.

- Representative variable

Usually, investigations that study TS or STVS, in order to distinguish stable and unstable profiles, use the variable that represents the type of stability under study, that is, the rotor angle (δ) in the case of TS, or the voltage magnitude (U) in the case of STVS. However, when both types of stability are considered, it is unclear which is the most appropriate variable to identify stable and unstable cases with the least or no margin error. In this sense, to determine this variable, tests of different fault cases are performed and the system's response is analyzed through SG rotor angles and IM voltage magnitudes, which are representative variables of TS and STVS, respectively.

Figure 5 shows the results obtained from eight fault cases under different operating scenarios, where it can be observed that through any of the two variables, (δ) o (U), it is possible to distinguish stable and unstable cases. Figure 5a shows the system response is stable for the first four fault cases, since after the disturbances, (U) remains within the allowed range of stability values; likewise, (δ) presents damped oscillatory characteristics that quickly stabilize. On the contrary, Figure 5b shows the system is unstable for the remaining four fault cases, as it presents a significant voltage drop with subsequent oscillations and a rapid growth of (δ) that exceeds the maximum limit of 180°.

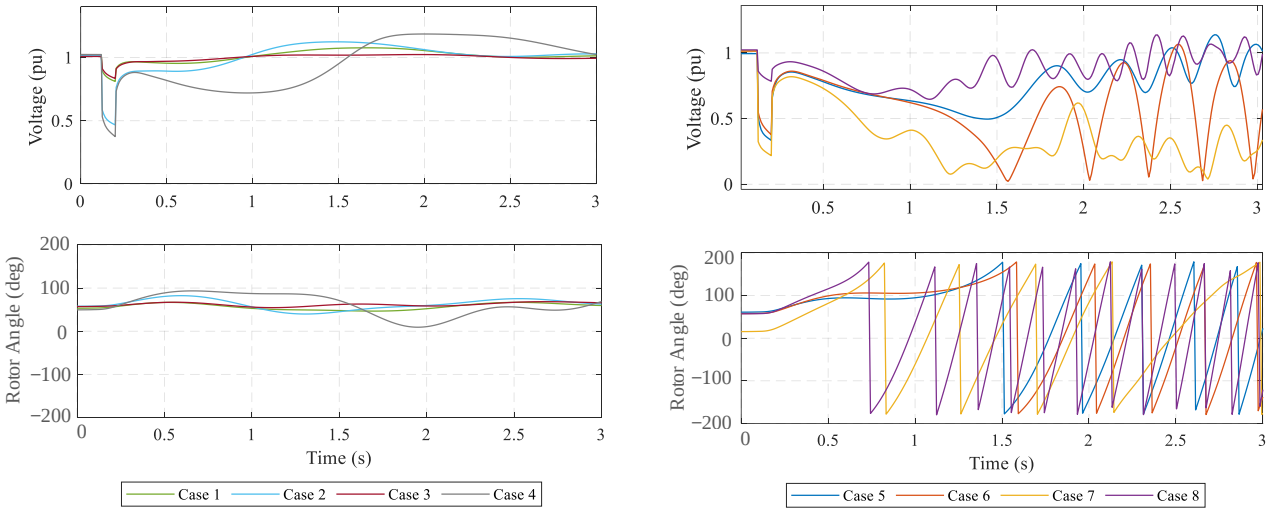

(**a**) (**b**)

Figure 5. U and δ responses after eight fault cases under different operating scenarios: (**a**) stable; (**b**) unstable.

Therefore, since short-term stability or instability is identified through either of the two variables (U o δ), this work selects the rotor angle trajectory (δ). This variable is selected because it is possible to use the maximum angular separation threshold after a contingency of 180°, where if any SG exceeds this threshold, the system is known to be unstable. On the contrary, the voltage magnitude does not present a defined threshold for the stability state. Therefore, the GS rotor angle trajectories are analyzed according to each GS's maximum angular separation criterion, with respect to the reference generator.

- Emergency control action application

As can be observed in Figure 5b, although it was possible to identify through any of the two variables (U or δ) that the system was unstable in the last four fault cases, it was impossible to recognize the dominant instability force in each case.

In this sense, the application of emergency control actions aimed at the possible instability mechanism, the IM load shedding or the SG tripping, is used. When IM load

shedding prevents instability development, it means that IM stalling is the dominant instability factor with the loss of STVS. On the contrary, when SG tripping mitigates instability development, the main mechanism causing instability corresponds to the SG out-of-synchronism with the loss of TS.

Therefore, by applying the mentioned control actions, it is possible to distinguish the type of instability of the last four unstable cases shown in Figure 5. First, the total IM load shedding is applied as a control action, and then the SG tripping with the greatest deviation in the rotor angle during the first moments after the fault clearance is applied. The control actions application is performed as quickly as possible before the instability development, while also considering the latencies that a control scheme implemented in real-time would imply. Figure 6 shows the system's response to these control actions.

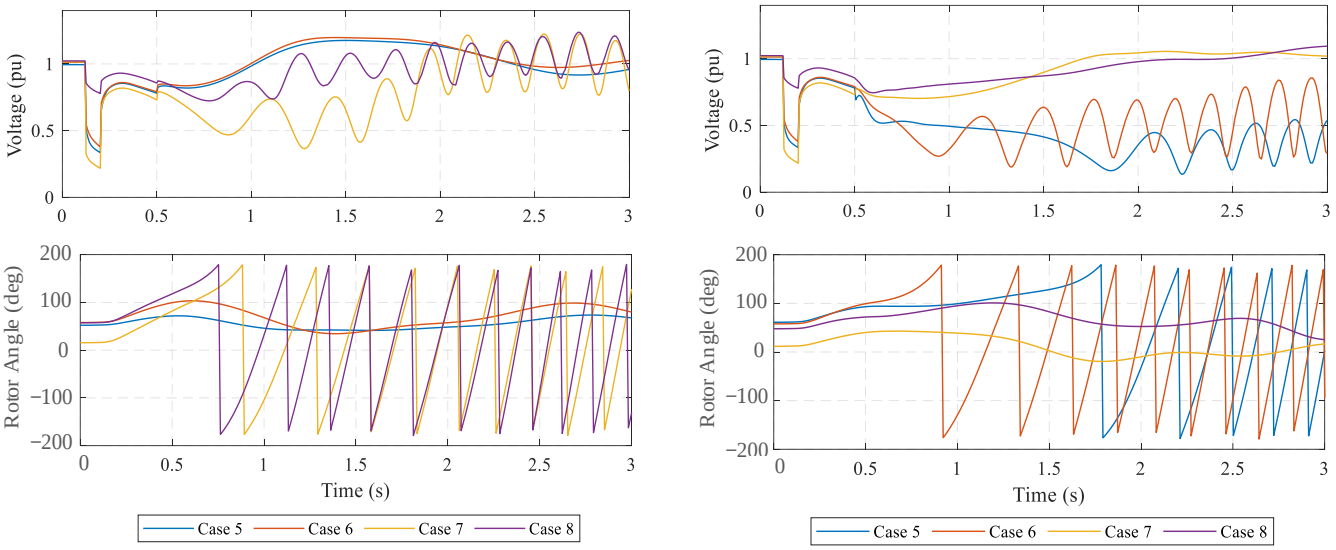

Figure 6. U and δ responses after the application of emergency control actions: (**a**) motor load shedding; (**b**) generation tripping.

As can be observed in Figure 6a, after the IM load shedding application, cases 5 and 6 show a stable response, while cases 7 and 8 remain unstable. On the contrary, after the SG tripping application, as shown in Figure 6b, cases 5 and 6 remain unstable, while cases 7 and 8 present a stable response. Therefore, it can be concluded that the dominant instability mechanism in cases 5 and 6 is the dynamic load with STVS loss, while in cases 7 and 8, it is the SG out-of-synchronism with TS loss. In addition, it can be noted that with only one control action type, it is possible to determine the dominant instability mechanism developed.

In this work, we decided to implement control actions that correspond to IM load shedding in whole cases found as unstable. That is, when these control actions prevent instability development, the STSS will be classified as unstable due to STVS. Otherwise, when the control actions have no effect on preventing the instability development, it means that the instability mechanism was not dynamic loading, but SG with rapid out-of-synchronism; therefore, the STSS is classified as unstable due to TS.

- STSS labeling summary

The STSS labeling process, as can be observed in Figure 7, is established in two stages. In the first stage, after setting simulation conditions related to the contingency and operation scenario, the initial load flow is executed and the time domain simulation is performed. Subsequently, the rotor angle response is monitored, where if the maximum angular separation between any generator with respect to the reference generator exceeds

the maximum theoretical limit of 180°, $|\Delta\delta|_{max} > 180°$, it means that one or more generators have lost synchronism and the voltage of different buses oscillates between high and low values. So, this case is defined as unstable, but the STSS classification is not precise, since the main instability mechanism is unknown. On the contrary, this case is considered stable when the $|\Delta\delta|_{max} < 180°$ throughout the simulation time.

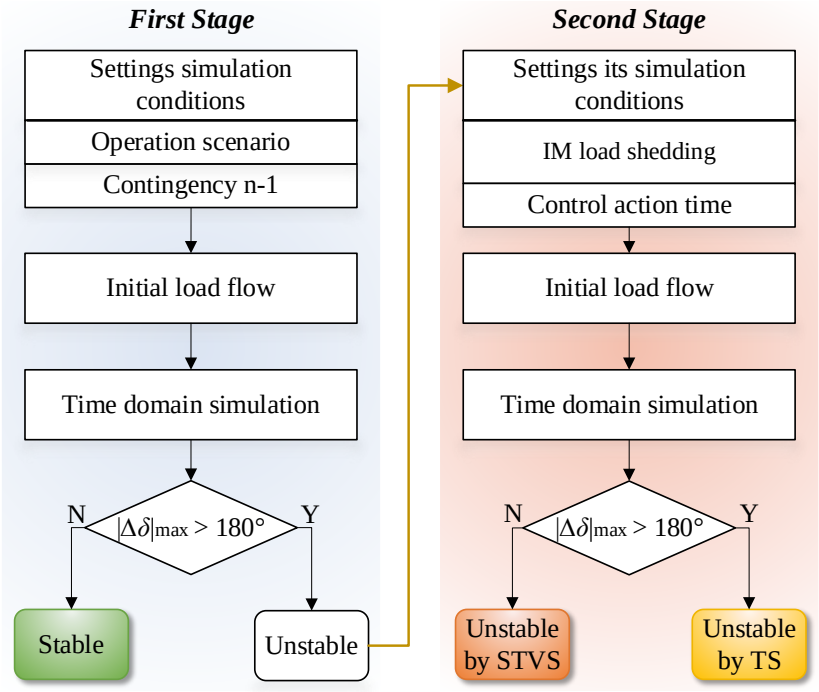

Figure 7. Flowchart of the defined STSS labeling.

Furthermore, the second stage aims to distinguish the main mechanism that leads to instability for the cases defined as unstable. For this, the application of total IM load shedding located in the buses with the highest IM concentration is added to the simulation conditions as an emergency control action, together with the execution time adjustment. The time setting used to execute the control action must consider the latencies involved in a load-shedding scheme when it is applied in real-time.

Finally, the initial load flow and the time domain simulation are executed. If the control action helps to recover the system, it means that the elements that led to instability were effectively dynamic loads; therefore, this case is classified as unstable due to STVS. On the contrary, when the application of the control action does not affect the system recovery, it means that the SGs play a more significant role in the instability development; therefore, this case is considered as unstable due to TS.

The STSS information defined by this methodology is represented by the vector c. This vector comprises three labels, each corresponding to the STSS (stable or unstable due to TS, or unstable due to STVS). Therefore,

$$c = \begin{cases} [1,0,0] & if \text{ STSS} = \text{stable} \\ [0,1,0] & if \text{ STSS} = \text{unstable by TS} \\ [0,0,1] & if \text{ STSS} = \text{unstable by STVS} \end{cases} \quad (2)$$

4.1.3. Database Generation: Summary

The STSS labeling methodology based on monitoring the rotor angle variable and the IM load shedding execution, as an action that indicates whether the problem is voltage instability, is used to classify the STSS in stable, unstable due to STVS, or unstable due to

TS systems. This classification methodology is developed under offline conditions using post-mortem analysis.

Once the STSS labeling information has been obtained, together with the time series of voltage phasors (U, θ) in each contingency, the RCNN model training is performed offline.

After the RCNN has been trained, it can be implemented in real-time. The input data required by the model will be the same as those used during its training, that is, the time series of voltage phasors, the variables measured directly by PMU devices.

4.2. Off-Line Training

Figure 4 shows the RCNN model training methodology aimed at assessing the STSS. As can be observed in this figure, model training requires an input database, which comprises the system's dynamic response in the face of different n-1 contingencies (simulation data or historical data) and the class to which each one belongs. On the one hand, the dynamic response is represented through the selected variables (U, θ); on the other hand, the class is acquired from the STSS labeling methodology.

Then, the RCNN training requires input data pre-processing to perform the classification task through spatial and temporal feature extraction, a particular property of the RCNN deep learning model.

4.2.1. Input Data Pre-Processing

The input data pre-processing involves the following steps: (a) selected variable (U, θ) organization in a format that the RCNN model can interpret; (b) input data splitting into two data sets called training and testing; (c) variable value normalization.

- Selected variable organization

Since the RCNN model is composed of convolution layers at the first hierarchical stage, the variables' data must be organized in a dimensional tensor that is analogous to images, that is, in a tensor of three axes. In the case of images, each axis represents the pixel height (h), the pixel width (w) and the color channels (usually three according to the RGB color coding); thus, the image tensor takes the form of $(h \times w \times 3)$. In this case, each axis represents the parameters that involve the selected variables (U, θ). The first axis corresponds to the sample number (T) within a given time window (W), starting from when the fault occurs until very shortly after the clearance. T is calculated from W and the sampling frequency f_s is calculated using $T = Wf_s + 1$. The second axis corresponds to the electrical system buses from which the selected variables are taken (B). Finally, the third axis considers the number of variables selected as input data, that is, two variables corresponding to the magnitude and angle of the voltage. Therefore, the RCNN input tensor has the form $(U, \theta) \in \mathbb{R}^{T \times B \times 2}$:

$$U = \begin{bmatrix} U_{1,1} & U_{1,2} & \cdots & U_{1,B} \\ U_{2,1} & U_{2,2} & \cdots & U_{2,B} \\ \vdots & \vdots & \ddots & \vdots \\ U_{T,1} & U_{T,2} & \cdots & U_{T,B} \end{bmatrix} \tag{3}$$

$$\theta = \begin{bmatrix} \theta_{1,1} & \theta_{1,2} & \cdots & \theta_{1,B} \\ \theta_{2,1} & \theta_{2,2} & \cdots & \theta_{2,B} \\ \vdots & \vdots & \ddots & \vdots \\ \theta_{T,1} & \theta_{T,2} & \cdots & \theta_{T,B} \end{bmatrix} \tag{4}$$

- Database splitting and normalization

The classification task involves splitting the database into the following two parts: the training dataset and test dataset. The information of each element of the training data set contains the class or label to which it belongs. In this way, when the training is performed, a model will be created based on the training data, which allows the class prediction of

each element of the test data set. The database splitting must be performed randomly and proportionally to each class.

Additionally, it is necessary to perform a normalization process due to the scale differences in the input characteristics, that is, in the selected variables (U, θ). For this purpose, the normalization algorithm called z-score is implemented, which ensures that each characteristic has a mean of 0 and a variance of 1.

4.2.2. RCNN Model Training

The RCNN model training process aims to find the learning parameters that minimize the difference between the model predictions and the classification states taken as true. For this purpose, the loss function and the optimization algorithm of the learning parameters play an essential role. On the one hand, the loss function measures the similarity between the network output predictions and the classification states taken as true. On the other hand, the optimization algorithm iteratively updates the learning parameters to minimize this loss function.

The cross-entropy (CE) function has been widely used as a loss function due to its good performance in multiclass classification tasks. However, in problems with unbalanced data sets, the classification process tends to pay too much attention to stable cases, which means that unstable cases suffer a loss of fit and generalization. Therefore, the loss function adopted for the RCNN model is an improved version of the CE function and is called weighted cross-entropy (WCE), which considers the class imbalance. WCE is defined by Equation (5).

$$Loss_1 = -\sum_i \alpha_i \left(\sum_j c_{i,j} log \widetilde{c}_{i,j} \right) \tag{5}$$

where α_i is the balance factor assigned to each class i. Normally, α_i of the unstable cases has a higher value (depending on its proportionality in the entire data set), so that the accuracy (ACC) for these cases increases. $(c_{i,1}, c_{i,2}, c_{i,3})$ are the STSS classes taken as true, while $(\widetilde{c}_{i,1}, \widetilde{c}_{i,2}, \widetilde{c}_{i,3})$ denotes the STSS prediction, that is, the output of the softmax function of the ith simulation case.

The WCE function is optimized through the Adam algorithm [38], which has been widely used in deep learning. Its application is adequate in the problem of STSS classification, since it produces excellent generalization results fairly rapidly.

4.2.3. Performance Metrics

Based on the confusion matrix in Table 2 used for binary classification problems, it is possible to adopt metrics such as accuracy (ACC), security (SS), reliability (CU) and G-mean, which allow the evaluation of the learning model performance. Although the RCNN model presents a multiclass classification problem, by considering each class i as binary subproblems, it is possible to perform the calculation of the mentioned metrics, as specified in Equations (6)–(9).

$$ACC = \frac{TP + TN}{TP + FP + TN + FN} \tag{6}$$

$$SS = \frac{\sum_{i=1}^{j} \frac{TP_i}{TP_i + FN_i}}{j} \tag{7}$$

$$CU = \frac{\sum_{i=1}^{j} \frac{TN_i}{TN_i + FP_i}}{j} \tag{8}$$

$$G - mean = \sqrt{SS \times CU} \tag{9}$$

where ACC is a widely used metric because it provides an overall measure of the proportion of correctly predicted samples. SS represents the proportion of correctly classified samples

within all stable samples. CU represents the proportion of correctly classified samples within all unstable samples, which reflects the reliability of the system assessment. Finally, G-mean is an appropriate metric to evaluate the classification of an unbalanced sample set, for example, when there are more stable than unstable samples [39].

Table 2. Confusion matrix for binary classification problems.

	Stable	**Unstable**
Predicted as stable	TP (true positive)	FP (false positive)
Predicted as unstable	FN (false negative)	TN (true negative)

4.3. Real-Time Application

The proposed methodology applied in real-time is shown in Figure 4. As can be observed, the methodology requires synchronized PMU measurements with a high sampling rate and an n-1 contingency alert for its activation. Then, it is necessary to prepare and pre-process the information obtained from the PMU measurements that correspond to the voltage phasors $(U,\ \theta)$, the variables used as input data in the RCNN training and are, therefore, required for its application in real-time. The preparation and pre-processing of $(U,\ \theta)$ measurements involve the following steps: (a) variable organization in a multi-dimensional tensor ($(U,\ \theta) \in \mathbb{R}^{T\times B\times 2}$); and (b) tensor normalization based on the same method (z-score) used offline. Subsequently, this information is delivered to the RCNN trained model that is capable of quickly classifying the system STSS. Based on the RCNN response, it is possible to guide emergency control actions, such as generation tripping or motor load shedding, when the model predicts instability caused by TS or instability by STVS, respectively.

The components required for STSS assessment based on the RCNN model in real-time correspond to a telecommunication system with high-speed characteristics that is necessary to transmit information from PMU devices to the control center, where the proposed methodology is implemented.

5. Simulation Results

The RCNN model was implemented in the New England 39-bus system, which has been modified from the original [40] to satisfy the N-1 security criteria. The database was generated based on time-domain simulations (TDS) in DIgSILENT® PowerFactory™, version 2021 SP2. The DL model was developed in Python version 3.8.8 using the libraries Keras 2.9.0 and Tensorflow 2.9.2 on a computer with Intel Core™ i7-9750H @ 2.60 GHz and 16 GB RAM.

5.1. Test System

The New England 39-bus system consists of 39 buses, 10 generators, 19 loads, and 46 transmission lines. The system is modeled considering the dynamics of both generation and loads. The generators use the 6th order sub-transient model equipped with automatic voltage regulators (AVR) and speed control regulators (GOV), which are models taken from the library of PowerFactory [41]. Likewise, in the case of loads, six induction motors were incorporated as dynamic loads through the IEEE Type 2 model located in the buses 4, 8, 15, 20, 24, and 28. Figure 8 shows the line diagram of this system.

The TDS consist of many case studies with N-1 contingencies, which are generated using the Monte Carlo method. Stable and unstable cases occur in these SDTs, where the driving force for unstable cases may be STVS loss or TS loss. In total, 10,000 study cases were generated, based on the following aspects:

- Variety in load/generation operation scenarios with the application of random N-1 contingencies.
- The contingencies correspond to generation output or three-phase faults located randomly on transmission lines, where the fault clearance occurs after 0.1 s.

- The simulation time window is established at 5 s, a time period in which the stability problems under study, STVS and TS, develop.
- The PMU sampling frequency can currently reach a value of 100/120 Hz; therefore, in this work, an integration step of 0.01 s is established.

The database size is considered to be sufficient due to the complexity of the RCNN model (number of learnable parameters) and the size selected by other AI-based studies that analyzed TS or STVS.

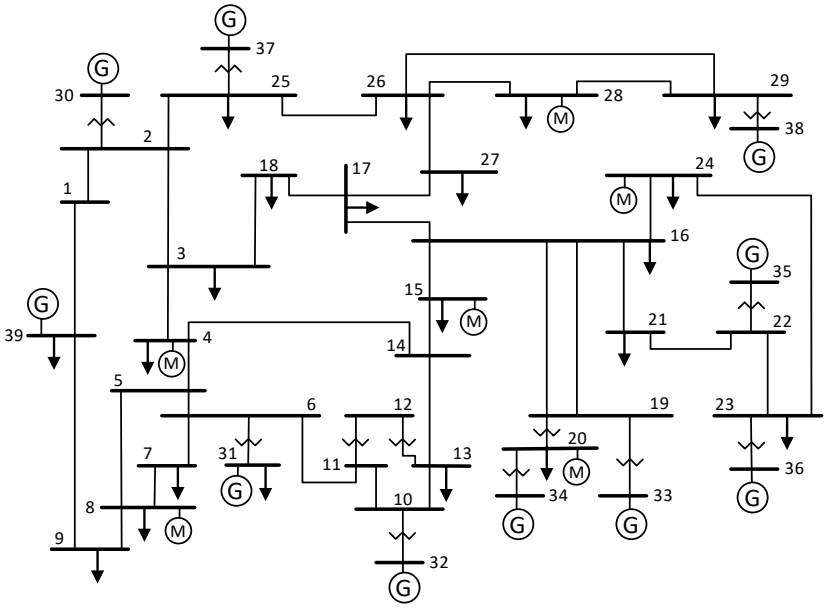

Figure 8. IEEE New England 39-bus system.

5.2. Off-Line STSS Assessment Results

The STSS assessment results are obtained through the methodology implementation outlined in Section 4.1.2, which consists of monitoring the SG rotor angle and applying emergency control actions that correspond to IM load shedding. The control action time delay was established based on the time a real-time control scheme would take [42,43]. In other words, this refers to a delay time that considers the latencies of (a) PMU data acquisition and communication system delay (~200 ms); (b) problem assessment based on AI (t_f + ~50 ms); (c) activation signal transfer from the control center to the local substations (<10 ms); circuit breaker operation (<40 ms). Therefore, the control action execution time is set to 400 ms from the start of the contingency, as the fault time (t_f) is 100 ms.

The STSS assessment results for the 10,000 study cases generated are presented in Table 3, where it can be observed that the system response is mostly stable with 8407 cases, unstable due to TS with 1178 cases, and finally, unstable due to STVS with 415 cases.

Table 3. Off-line STSS assessment results.

STSS	Number of Cases	Percentage
Stable	8407	84%
Unstable due to TS	1178	12%
Unstable due STVS	415	4%

In the literature, it can be observed that other methods to classify stable and unstable cases in the study of TS or STVS have been widely used, where the maximum Lyapunov exponent (MLE) estimation stands out. The MLE approach is based on trajectory behavior analysis, where the exponential variations experienced by a power system in the transient process are quantified [44]. When the MLE sign is positive, it means that there is an

exponential divergence problem with an unstable system response. In this sense, for comparative purposes with the proposed classification methodology (PCM), we decided to analyze, based on the MLE approach, the voltage magnitude values from all buses in the study cases to classify STSS as stable or unstable. When the MLE sign is negative for all buses, the system is identified as stable; otherwise, when at least one bus is positive, the system is classified as unstable. Table 4 summarizes the STSS assessment results (stable and unstable) for the 10,000 study cases based on MLE and PCM.

Table 4. STSS assessment results based on MLE and PCM.

STSS	PCM		MLE	
	# Cases	(%)	# Cases	(%)
Stable	8407	84	8238	82
Unstable due to TS	1178	16	1762	18
Unstable due to STVS	415			

As can be observed in Table 4, the classification results for PCM and MLE are very similar, with 84% and 82% stable cases, and 16% and 18% unstable cases, that is, only a 2% difference between both methodologies. However, it is known that the MLE will always present a classification error margin, since its calculation is based on numerical methods. In this sense, although the MLE has been a useful tool to discriminate between stable and unstable profiles, it has several limitations, such as the error associated with its classification, the lack of ability to explain the dominant instability factor, and also its heavy theoretical basis. Therefore, the PCM has a clear implementation advantage, since it not only allows for STSS classification, including the dominant instability mechanism, but also accomplishes this purpose without the development of complex algorithms and a significant computational effort.

5.3. RCNN Training

RCNN model training requires input data pre-processing and the adjustment of its design. The procedure for performing the model training is detailed below.

5.3.1. Input Data and Pre-Processing

The RCNN input database comprises a time series of the voltage magnitude and voltage angle $(U,\ \theta)$ of all the system buses within a very short time window from the fault occurrence.

Based on the time delay considered in Section 5.2 that corresponds to the problem assessment using learning models, $t_f + 50$ ms, it was established that the time window (W) is $t_f + 40$ ms, i.e., $W = 100$ ms $+ 40$ ms $= 140$ ms, where 10 ms is reserved for calculations that imply the methodology application in real-time. Once W is defined and considering a sampling frequency $f_s = 100$ Hz, the sample number T associated with the time window results in $T = 0.14 \times 100 + 1 = 15$. Therefore, the RCNN input tensor is $(U,\ \theta) \in \mathbb{R}^{15\times39\times2}$ in each contingency.

Then, the entire database was divided into the following three parts: training (60% ≡ 6000 cases), validation (20% ≡ 2000 cases), and testing (20% ≡ 2000 cases), where the percentage of stable cases, unstable due to TS, and unstable due to STVS in each data set has the same proportionality.

Additionally, the database must undergo a normalization process before the model is trained due to the scale difference between the model characteristics. Therefore, as indicated in Section 4.2.1, data set normalization is performed by the z-score algorithm.

5.3.2. RCNN Model Design

Based on the design of deep learning models aimed at studies of transient or voltage stability and at achieving good classification performance in the learning process, the

architecture design shown in Figure 9 was obtained. The hyperparameters adjusted in this figure correspond to the number of convolutional layers, in addition to the size and number of filters, max pooling operation, dropout probability, number of LSTM layers, number of fully connected (FC) layers, activation functions, and finally, normalization layers.

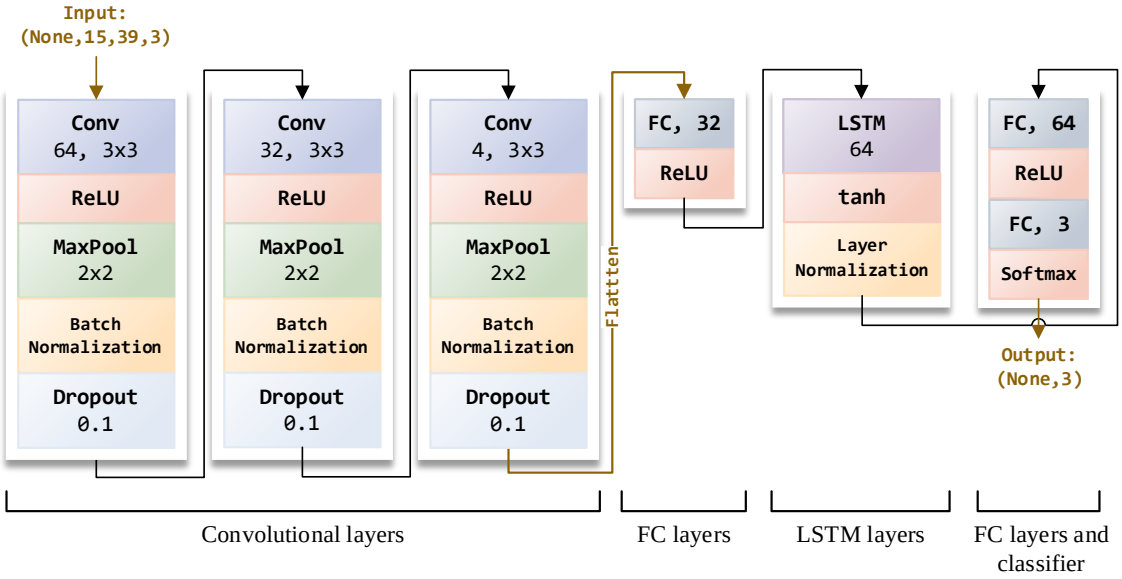

Figure 9. RCNN model design.

Additionally, the hyperparameters related to loss function, the optimization algorithm, initialization technique, batch size, and epoch number must be adjusted to perform the model training. Table 5 summarizes the settings for these hyperparameters.

Table 5. RCNN hyperparameter settings.

Training Hyperparameters	Function/Selected Values
Loss function	Weighted cross-entropy (WCE), α= (0.4, 2.8, 8.0)
Optimization algorithm	Adam algorithm, learning rate = 0.0001
Initialization technique	Glorot uniform
Batch size	120
Epoch number	2000

As can be observed in Table 5, the WCE loss function adds a balance factor of α among all classes according to the assignment of weight, which is determined as $\alpha_j = n/kn_j$, where α_j is the weight of class j, n is the total number of study cases (10,000), n_j is the number of j class study cases (stable: 8407, unstable due to TS; 1178, unstable due to STVS: 415), and k is the total number of classes (3).

5.3.3. Training Process

The training process determines the weights of each layer that comprises the RCNN model, where the multidimensional input data are clustered according to the corresponding classification class. The t-distributed stochastic neighbor embedding (tSNE) technique allows the visualization of this classification process through the use of its non-linear dimensionality reduction feature to aggregate high-dimensional data in a two- or three-dimensional space [45]. In this sense, in order to observe the clustering process of the multidimensional input data during the model training, the t-SNE technique is used in the following three different locations: (a) input space, before entering the model; (b) output of

the hierarchical convolutional module; and (c) after the LSTM module, before the last fully connected layer. Figure 10 shows the RCNN learning process in a scatter plot, where the sample point clustering of the input database in each indicated position can be observed, representing the stability state class by means of colors, and the sample points' proximity through the similarities that can be observed among them.

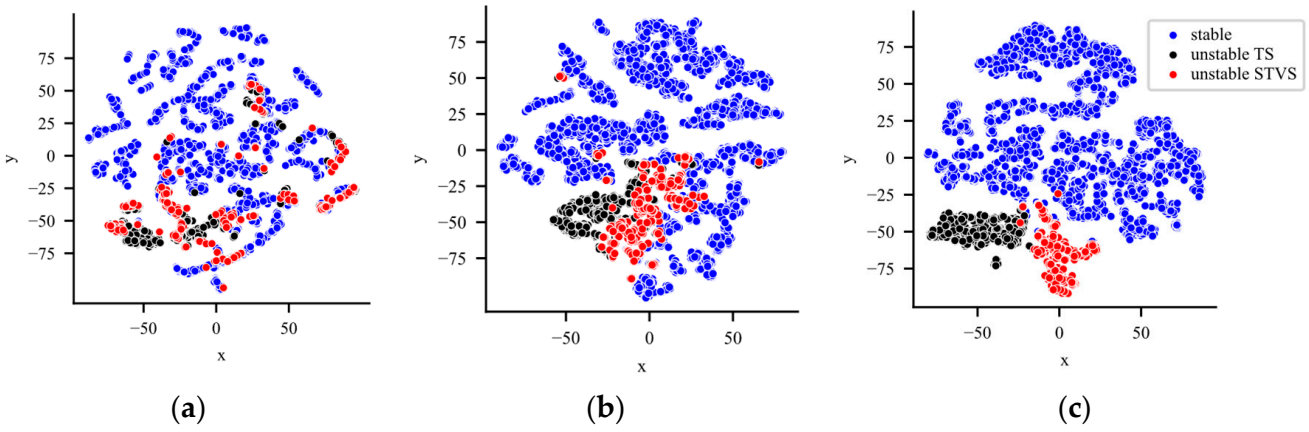

Figure 10. RCNN learning process visualization. (**a**) Sample points in the input space. (**b**) Sample points in the CNN module output space. (**c**) Sample points in the output space of the penultimate FC layer.

It can be observed in Figure 10a that the stability classes overlap with each other because the RCNN model has not yet processed the data set. This changes significantly in Figure 10b as the dataset has already been processed by the hierarchical convolutional module, where a clustering of the three stability classes can be distinguished to some extent, which demonstrates the module's great ability to extract spatial features. In addition, in Figure 10c, it can be observed that the clustering of the three stability classes is much more evident, since, at this stage, the data set has also been processed by the LSTM module, which verifies the importance of temporal feature extraction for a more precise classification of STSS.

5.3.4. RCNN Results and Comparison with Other Models

The RCNN and other ML models' performance results for the test data set are shown in Table 6. The models correspond to (1) SVM (support vector machines); (2) MLP (multilayer perceptron), whose hidden layer size is 390 neurons; (3) LSTM with a setting of 128 neurons as its memory unit; and (4) CNN with 3 hidden layers composed of 64, 32, and 4 filters and common size of 3×3.

Table 6. Metrics comparison among different models.

Model	ACC (%)	SS (%)	CU (%)	G-Mean (%)
SVM	91.80	95.44	91.80	93.60
MLP	93.87	96.07	93.87	94.96
LSTM	95.73	96.94	95.73	96.33
CNN	96.47	97.34	96.46	96.90
RCNN	98.13	98.33	98.07	98.20

It can be observed from Table 6 that the traditional ML methods, SVM and MLP, have the lowest performance metrics, with values between 91% and 94%. Deep learning methods such as LSTM and CNN can significantly improve these metrics. The DL methods show a performance increase of at least 1.37% in ACC and G-mean, where CNN is the singular DL method that presents the best performance. However, although LSTM and CNN show evidence of great performance, their metrics are lower when a hybrid DL model that combines the capabilities of extracting temporal and spatial features, such as the RCNN model, is implemented. The performance metric results obtained from the RCNN are much

better than for the ML and DL methods, with a significant increase of 1.3% in G-mean, proving the advantage of combining singular DL capabilities from CNN and LSTM.

Additionally, the RCNN model training process's efficiency was compared with the other three deep learning models based on neural networks (MLP, LSTM, and CNN). Figure 11 shows the validation curves during the training epochs.

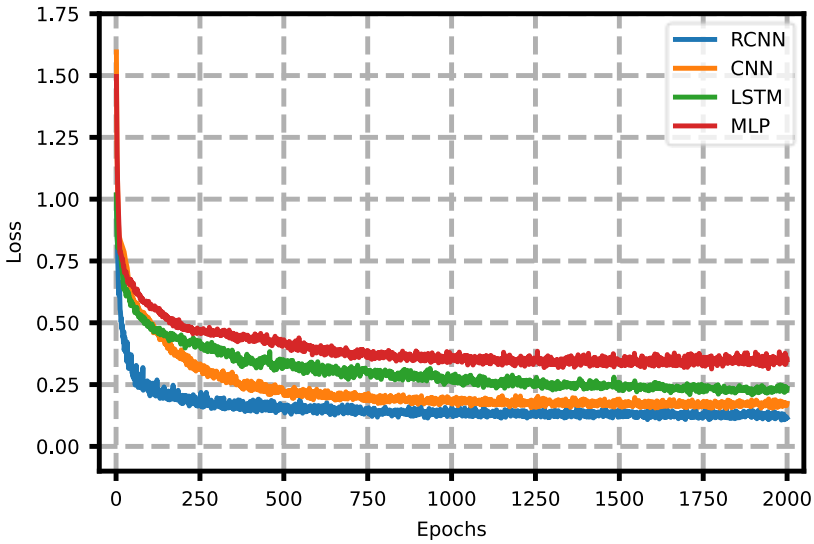

Figure 11. Loss comparison of the validation data sets among different learning models.

It can be observed in Figure 11 that the RCNN loss minimization is the smallest compared to the other models and the RCNN also presents a faster convergence rate with a smaller number of epochs. Therefore, the RCNN model, in addition to providing excellent performance metrics, involves a training process that is more efficient compared to the other learning models based on neural networks.

5.4. Robustness Analysis

5.4.1. Measurement Loss

The RCNN performance results are based on the assumption that measurements from all buses are always available. However, some measurements may be missing in practice due to measurement loss, delay, or communication loss. In this sense, the RCNN performance is analyzed while considering the unavailability of measurements for different buses.

As there may be information redundancy in the measurements from all system buses, the measurement from one or more missing buses can be estimated based on other available information, for example, by state estimation. In order to simplify and accelerate the calculations when the model is applied in real-time, in this work, the missing measurement of any bus is calculated simply through the average value of the adjacent buses' measurements. Although this calculation may seem inaccurate, tests have shown that a model trained with complete data can tolerate this error and achieve great performance.

In this sense, for all P-1 loss scenarios (if the voltage phasor of any one bus is not available), in the test data set, the missing measurements of each bus are calculated as the average values of the adjacent buses. Then, the RCNN model is evaluated with the modified data and the performance results can be observed in Figure 12 through the representative metric G-mean.

As can be observed in Figure 12, the RCNN performance is greater than 96% in any case of loss of measurements (P-1). In addition, it can be noted that there is a particular decrease in performance when a measurement loss is reported for buses 19, 20, 23, 24, and 28, where some MI are located, and for buses 33 to 39, where some synchronous generators are located. Therefore, it can be affirmed that the measurements for the motor load and

generation buses are of fundamental importance to achieve great performance in RCNN classification tasks.

This approach could also be used when there is a greater measurement loss. In this case, it is shown that the RCNN model under P-1 loss scenarios can yield great performance simply by using the average values of the adjacent buses for the missing information. A slight decrease in performance demonstrates the excellent robustness against the measurement loss in the STSS assessment.

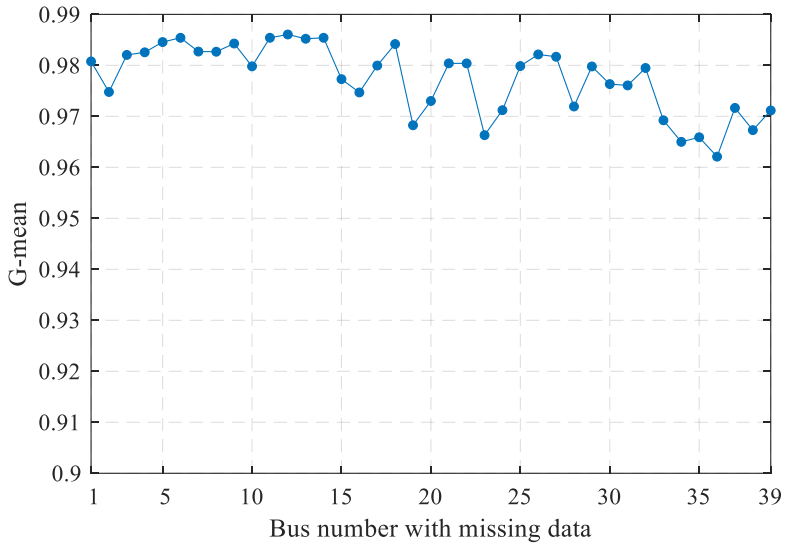

Figure 12. G-mean metric results for missing PMU data.

5.4.2. Noise

Once the model is applied in real-time, the input damage problem led by load fluctuation or poor measurement must be considered. In this sense, the signal/noise ratio (SNR) is used in the RCNN input data.

When the SNR has small values, it means that there is a high distortion of the signal. Thus, the RCNN performance under different SNR values was evaluated using the test data set. Table 7 summarizes the performance results obtained under these distortion conditions for the model input data.

Table 7. RCNN metrics under noise conditions.

Noise Conditions		ACC	SS	CU	G-Mean
Ideal		98.13	98.33	98.07	98.20
SNR (dB)	40	97.84	97.94	97.68	97.81
	30	97.15	97.35	97.09	97.22
	20	96.73	96.86	96.54	96.70

As can be observed in Table 7, the metrics present a slight decrease when the SNR has large values, including 40 dB. On the contrary, when it is assumed that the SNR = 20 dB, the metrics CU and G-mean decrease by around 1.5%. Therefore, the model demonstrates competitive performance under large noise interference. It is worth mentioning that the SNR values analyzed are fairly demanding, since the noise levels recorded by PMU using its different measurement signals are much lower, around 70–80 dB, which means that despite considering extreme noise conditions in all PMU measurement signals, the RCNN model is capable of great classification performance.

5.5. Sensibity Analysis

The RCNN model was developed using input data under different conditions, such as a certain time window and data from all power system buses. Sensitivity analysis was performed when the RCNN was trained under different conditions on its input data in order to verify that the established conditions result in the best performance of the model.

5.5.1. Time-Window Length

The time window (W) was established based on the latencies involved in executing automatic control actions and considering the average assessment delay required by learning models. In this sense, W was established as 140 ms, a time that includes fault duration, where the performance results were excellent at around 98%. However, to verify that the established time-window length could achieve the highest performance metrics, systematic training tests with different values of time-window length were performed. The tests included the following values: 100 ms (11 samples considering only t_f), 110 ms (12 samples), 120 ms (13 samples), 130 ms (14 samples), and 140 ms (15 samples, which was the time window initially set). Table 8 shows the performance metrics results with the mentioned changes in time-window length.

Table 8. Metrics comparison among different time-window lengths.

W (Samples Number)	ACC (%)	SS (%)	CU (%)	G-Mean (%)
100 ms (11)	95.34	95.23	95.44	95.34
110 ms (12)	95.80	95.70	96.84	96.27
120 ms (13)	96.27	96.17	97.31	96.74
130 ms (14)	97.42	97.31	98.47	97.89
140 ms (15)	98.13	98.33	98.07	98.20

As shown in Table 8, as the time-window length increases, the performance metrics tend to increase, especially when the time-window length is greater than the fault time. The highest performance metrics, which exceed 97%, have a window length of 130 ms and 140 ms. Although a window length of 130 ms provides more time for emergency control action execution, the 140 ms window is preferred, since this time also allows the execution of control actions and additionally presents the best performance over all other cases.

The results also show that the minimum performance obtained is around 95% in all metrics, i.e., under a data window with only the fault time, the RCNN model has competitive performance. In addition, this model based on deep learning does not require information about the contingency (type, location, and magnitude) or the system operation state. Therefore, it is evident that the RCNN single application, even with the worst conditions in the input data set during the training process, is superior and has significant advantages.

5.5.2. Input Data Location

The RCNN model was developed assuming that voltage phasor measurement data for all system buses are always available; however, systems generally do not have all measurements available in practice. In this sense, the RCNN is trained with only data on generation and motor load buses, in which the short-term instability mechanisms are more closely reflected.

In this context, as the test system has 10 generation buses and 6 IM load buses, instead of considering 39 buses for the input tensor dimension setting, only 16 generation and load buses are considered, which results in a dimension tensor of $(U,\ \theta,\ \omega) \in \mathbb{R}^{15\times16\times2}$ in each contingency. Additionally, tests are also performed when there are only measurements on generation buses with a dimension tensor of $(U,\ \theta,\ \omega) \in \mathbb{R}^{15\times10\times2}$, and measurements on IM load buses with a dimension tensor of $(U,\ \theta,\ \omega) \in \mathbb{R}^{15\times6\times2}$ available. Table 9 summarizes the performance results for the test data set.

Table 9. RCNN performance metrics with measurements of generation and/or motor load buses.

Measurements	ACC	SS	CU	G-Mean
Total (39 B)	98.13	98.33	98.07	98.20
GS-MI (16 B)	97.38	95.93	98.94	97.42
GS (10 B)	91.57	89.47	93.94	91.68
MI (6 B)	93.46	92.63	94.03	93.33

As can be observed in Table 9, when the RCNN is trained only with generation and motor load buses, the metrics performance decreases by a small percentage of 0.8% compared to the model trained using the total measurements. Therefore, the importance of the bus data located in elements associated with the types of stability under study, i.e., SG and IM, is evident.

However, when the model is trained only with generation buses or IM load buses, the model performance noticeably decreases by around 5–7%.

Therefore, when a power system has limited measurements, it is recommended that the available PMU is found in generation and dynamic load buses, where the short-term stability problems are directly reflected. Then, excellent results can be achieved following the training of the learning model with these data and the STSS prediction.

5.6. Real-Time Application

The RCNN real-time application requires PMU information to be pre-processed, meaning that it is organized and normalized, so that the trained RCNN model can classify the STSS. Figure 13 shows the total timeline required for RCNN real-time application, from fault occurrence to STSS classification. It can be observed in this figure that the delay time is 343.7 ms, which considers the selected time-window length (140 ms), the computational processing time (3.7 ms), and the PMU data acquisition, together with the system communication delay (200 ms). This time, which includes the fault duration, is quite fast and ensures emergency control actions have the time to mitigate instability cases. This is demonstrated in Figure 14, where an unstable case and the real-time model's delay are shown. Time (1) is the total delay of 343.7 ms, and time (2) is the time remaining between the classification result and the collapse, where an automatic control scheme has the necessary time to execute an emergency control action and prevent instability propagation in the system.

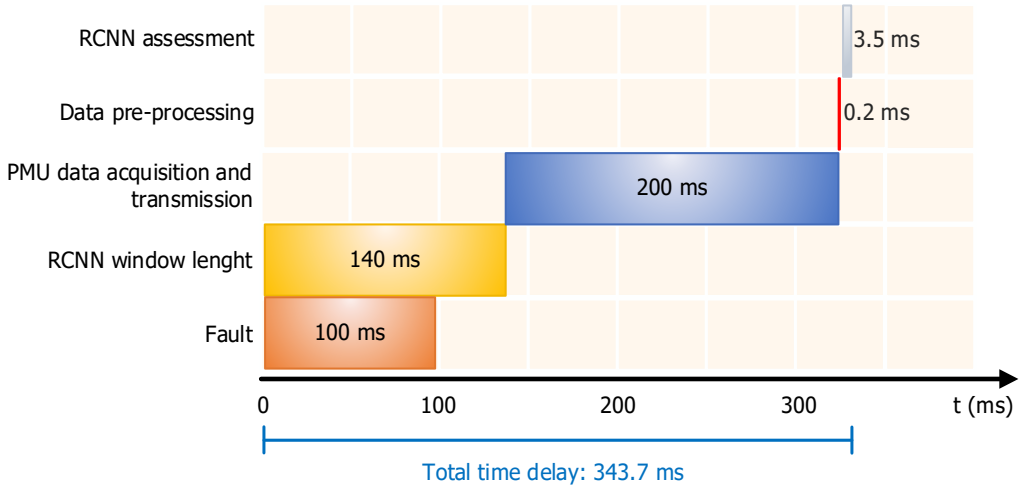

Figure 13. Time delay summary for RCNN real-time application.

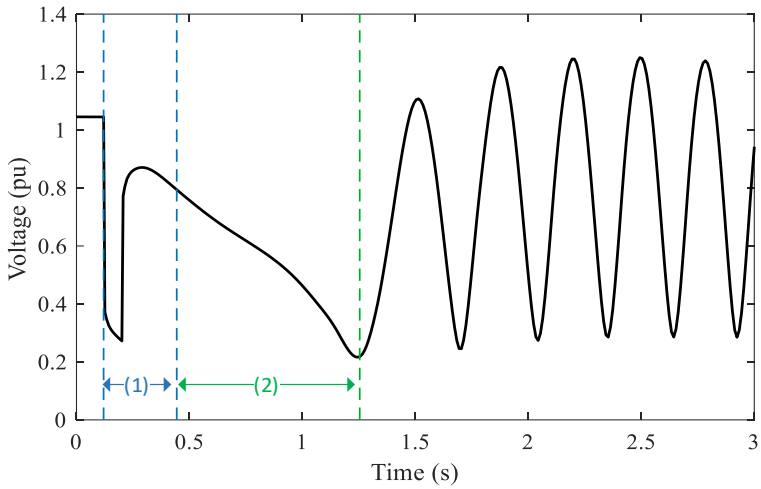

Figure 14. RCNN time delay in real-time for an unstable study case. (1) Total delay time assessment. (2) Remaining time between assessment result and unstable condition.

5.7. Discussion Results

The proposed methodology based on the combination of deep learning methods has advantages not only in the joint assessment of TS and STVS with a high-performance degree above 98%, but also in the predictive assessment that can take place before instability occurs. These aspects are of fundamental importance for automatic control actions, since they are required to be effective through their orientation to the main driving force of instability and executed in time before the development of instability, thus being able to avoid the instability propagation in the electrical system.

On the other hand, throughout this work, the methodology developed for the joint assessment of TS and STVS has been implemented in an electrical system composed only of synchronous generators as energy sources. However, this does not mean that the methodology presents restrictions for systems with renewable power generation, such as wind or solar, since it would only be necessary to obtain a database under the new generation conditions with the corresponding STSS labeling. This is the necessary information for deep learning RCNN training and its subsequent real-time application.

6. Conclusions

This work proposes the joint assessment of transient and short-term voltage stability to address the early warning of the short-term stability state (STSS) in stable or unstable due to SG out-of-synchronism, or unstable due to IM stalling, based on the RCNN deep learning model and WAMS-PMU measurements. The work develops a novel STSS offline classification methodology based on analyzing the SG rotor angle trajectories and applying emergency control actions directed towards the instability mechanism. The classification results, together with the time series information of the voltage's magnitude and angle, allow the deep neural network RCNN training, which is capable of automatically capturing spatial and temporal features of the database and predictively classifying the STSS with a high degree of performance when the RCNN is applied in real-time. The proposed methodology was implemented in the New England 39-bus system, where a series of studies and comparisons with other traditional and deep learning models were exhaustively performed. The results showed that the RCNN performance is at least 2% higher than the other learning methods; in addition, it has a competitive performance of over 97% when the model uses measurement data only from generation and dynamic load buses. Likewise, it was demonstrated that the delay time associated with the real-time application of the RCNN (343.7 ms, including the fault duration time) allows the guidance and execution of effective emergency control actions that prevent system instability development.

In future work, research must be directed at diagnosing the system elements that cause instability after a fault; therefore, it will be possible to develop a control scheme that avoids instability development with minimal element shedding.

Author Contributions: Conceptualization, E.A.T. and D.G.C.; methodology, E.A.T. and D.G.C.; software, E.A.T.; validation, E.A.T., D.G.C. and J.L.R.T.; formal analysis, E.A.T. and D.G.C.; investigation, E.A.T.; resources, E.A.T. and D.G.C.; data curation, E.A.T. and D.G.C.; writing—original draft preparation, E.A.T.; writing—review and editing, E.A.T., D.G.C. and J.L.R.T.; visualization, E.A.T.; supervision, D.G.C. and J.L.R.T. All authors have read and agreed to the published version of the manuscript.

Funding: This work was supported in part by the German Academic Exchange Service (Deutscher Akademischer Austauschdienst—DAAD) under the program Third Country Programme Latin America and National Council for Scientific and Technical Research of Argentina (CONICET) under the program PhD Completion Scholarship.

Conflicts of Interest: The authors declare no conflict of interest.

References

1. Taylor, C.W. *Power System Voltage Stability*; McGraw-Hill: New York, NY, USA, 1994.
2. Pavella, M.; Murthy, P.G. *Transient Stability of Power Systems: Theory and Practice*; U.S. Department of Energy: Washington, DC, USA, 1994.
3. Glavic, M.; Novosel, D.; Heredia, E.; Kosterev, D.; Salazar, A.; Habibi-Ashrafi, F.; Donnelly, M. See It Fast to Keep Calm: Real-Time Voltage Control Under Stressed Conditions. *IEEE Power Energy Mag.* **2012**, *10*, 43–55. [CrossRef]
4. Gomez, F.R.; Rajapakse, A.D.; Annakkage, U.D.; Fernando, I.T. Support vector machine-based algorithm for post-fault transient stability status prediction using synchronized measurements. *IEEE Trans. Power Syst.* **2010**, *26*, 1474–1483. [CrossRef]
5. Hou, K.; Shao, G.; Wang, H.; Le Zheng, L.; Zhang, Q.; Wu, S.; Hu, W. Research on practical power system stability analysis algorithm based on modified SVM. *Prot. Control. Mod. Power Syst.* **2018**, *3*, 1–7. [CrossRef]
6. Zhang, Y.; Xu, Y.; Bu, S.; Dong, Z.Y.; Zhang, R. Online power system dynamic security assessment with incomplete PMU measurements: A robust white-box model. *IET Gener. Transm. Distrib.* **2019**, *13*, 662–668. [CrossRef]
7. Tongwen, W.; Lin, G. A data mining technique based on pattern discovery and k-nearest neighbor classifier for transient stability assessment. In Proceedings of the 2007 International Power Engineering Conference (IPEC 2007), Singapore, 3–6 December 2007; pp. 118–123.
8. Zhang, Y.; Xu, Y.; Dong, Z.Y.; Xu, Z.; Wong, K.P. Intelligent Early Warning of Power System Dynamic Insecurity Risk: Toward Optimal Accuracy-Earliness Tradeoff. *IEEE Trans. Ind. Inform.* **2017**, *13*, 2544–2554. [CrossRef]
9. Ren, C.; Xu, Y.; Zhang, Y. Post-disturbance transient stability assessment of power systems towards optimal accuracy-speed tradeoff. *Prot. Control. Mod. Power Syst.* **2018**, *3*, 19. [CrossRef]
10. Xu, Y.; Dong, Z.Y.; Zhao, J.H.; Zhang, P.; Wong, K.P. A Reliable Intelligent System for Real-Time Dynamic Security Assessment of Power Systems. *IEEE Trans. Power Syst.* **2012**, *27*, 1253–1263. [CrossRef]
11. Pinzón, J.D.; Colomé, D.G. Real-time multi-state classification of short-term voltage stability based on multivariate time series machine learning. *Int. J. Electr. Power Energy Syst.* **2019**, *108*, 402–414. [CrossRef]
12. Goodfellow, I.; Bengio, Y.; Courville, A. *Deep Learning*; MIT Press: Cambridge, MA, USA, 2016.
13. Zhu, Q.; Chen, J.; Li, H.; Shi, D.; Li, Y.; Duan, X. Transient stability assessment based on stacked autoencoder. In Proceedings of the CSEE, Budapest, Hungary, 8–10 April 2018; Volume 38, pp. 2937–2946.
14. Yu, J.J.Q.; Hill, D.J.; Lam, A.Y.S.; Gu, J.; Li, V.O.K. Intelligent Time-Adaptive Transient Stability Assessment System. *IEEE Trans. Power Syst.* **2017**, *33*, 1049–1058. [CrossRef]
15. Yu, J.J.; Hill, D.J.; Lam, A.Y. Delay aware transient stability assessment with synchrophasor recovery and prediction framework. *Neurocomputing* **2018**, *322*, 187–194. [CrossRef]
16. Zhu, L.; Hill, D.J.; Lu, C. Hierarchical Deep Learning Machine for Power System Online Transient Stability Prediction. *IEEE Trans. Power Syst.* **2019**, *35*, 2399–2411. [CrossRef]
17. Shi, Z.; Yao, W.; Zeng, L.; Wen, J.; Fang, J.; Ai, X.; Wen, J. Convolutional neural network-based power system transient stability assessment and instability mode prediction. *Appl. Energy* **2020**, *263*, 114586. [CrossRef]
18. Zhu, L.; Hill, D.J.; Lu, C. Intelligent Short-Term Voltage Stability Assessment via Spatial Attention Rectified RNN Learning. *IEEE Trans. Ind. Inform.* **2020**, *17*, 7005–7016. [CrossRef]
19. Zhong, Z.; Guan, L.; Su, Y.; Yu, J.; Huang, J.; Guo, M. A method of multivariate short-term voltage stability assessment based on heterogeneous graph attention deep network. *Int. J. Electr. Power Energy Syst.* **2021**, *136*, 107648. [CrossRef]
20. Huang, J.; Guan, L.; Su, Y.; Yao, H.; Guo, M.; Zhong, Z. Recurrent Graph Convolutional Network-Based Multi-Task Transient Stability Assessment Framework in Power System. *IEEE Access* **2020**, *8*, 93283–93296. [CrossRef]
21. Wang, G.; Zhang, Z.; Bian, Z.; Xu, Z. A short-term voltage stability online prediction method based on graph convolutional networks and long short-term memory networks. *Int. J. Electr. Power Energy Syst.* **2020**, *127*, 106647. [CrossRef]

22. Ge, H.; Guo, Q.; Sun, H.; Zhao, W. A model and data hybrid-driven short-term voltage stability real-time monitoring method. *Int. J. Electr. Power Energy Syst.* **2019**, *114*, 105373. [CrossRef]
23. Wang, Y.; Sun, Y.; Mei, S. A method of distinguishing short-term voltage stability from rotor angle stability and its application. *IEEE PES Innov. Smart Grid Technol.* **2012**, 1–5. [CrossRef]
24. Han, T.; Chen, Y.; Ma, J.; Zhao, Y.; Chi, Y.-Y. Surrogate Modeling-Based Multi-Objective Dynamic VAR Planning Considering Short-Term Voltage Stability and Transient Stability. *IEEE Trans. Power Syst.* **2017**, *33*, 622–633. [CrossRef]
25. Lashgari, M.; Shahrtash, S.M. Fast online decision tree-based scheme for predicting transient and short-term voltage stability status and determining driving force of instability. *Int. J. Electr. Power Energy Syst.* **2021**, *137*, 107738. [CrossRef]
26. Kundur, P.; Paserba, J.; Ajjarapu, V.; Andersson, G.; Bose, A.; Canizares, C.; Hatziargyriou, N.; Hill, D.; Stankovic, A.; Taylor, C.; et al. Definition and Classification of Power System Stability IEEE/CIGRE Joint Task Force on Stability Terms and Definitions. *IEEE Trans. Power Syst.* **2004**, *19*, 1387–1401.
27. Machowski, J.; Lubosny, Z.; Bialek, J.W.; Bumby, J.R. *Power System Dynamics: Stability and Control*; John Wiley & Sons: New York, NY, USA, 2020.
28. van Cutsem, T.; Vournas, C. *Voltage Stability of Electric Power Systems*; Springer Science & Business Media: New York, NY, USA, 2007.
29. Bai, H.; Ajjarapu, V. A Novel Online Load Shedding Strategy for Mitigating Fault-Induced Delayed Voltage Recovery. *IEEE Trans. Power Syst.* **2010**, *26*, 294–304. [CrossRef]
30. Potamianakis, E.; Vournas, C. Short-Term Voltage Instability: Effects on Synchronous and Induction Machines. *IEEE Trans. Power Syst.* **2006**, *21*, 791–798. [CrossRef]
31. Liu, C.-L.; Hsaio, W.-H.; Tu, Y.-C. Time Series Classification With Multivariate Convolutional Neural Network. *IEEE Trans. Ind. Electron.* **2018**, *66*, 4788–4797. [CrossRef]
32. Massaoudi, M.; Abu-Rub, H.; Refaat, S.S.; Chihi, I.; Oueslati, F.S. Deep Learning in Smart Grid Technology: A Review of Recent Advancements and Future Prospects. *IEEE Access* **2021**, *9*, 54558–54578. [CrossRef]
33. Zhang, W.J.; Yang, G.; Lin, Y.; Ji, C.; Gupta, M.M. On definition of deep learning. In Proceedings of the 2018 World Automation Congress (WAC), Washington, DC, USA, 3–6 June 2018; pp. 1–5.
34. Schmidhuber, J.; Hochreiter, S. Long short-term memory. *Neural Comput.* **1997**, *9*, 1735–1780.
35. Yamashita, R.; Nishio, M.; Do, R.K.G.; Togashi, K. Convolutional neural networks: An overview and application in radiology. *Insights Imaging* **2018**, *9*, 611–629. [CrossRef] [PubMed]
36. Rajapakse, A.D.; Gomez, F.; Nanayakkara, K.; Crossley, P.A.; Terzija, V.V. Rotor angle instability prediction using post-disturbance voltage trajectories. *IEEE Trans. Power Syst.* **2009**, *25*, 947–956. [CrossRef]
37. Zhang, R.; Xu, Y.; Dong, Z.Y.; Wong, K.P. Post-disturbance transient stability assessment of power systems by a self-adaptive intelligent system. *IET Gener. Transm. Distrib.* **2015**, *9*, 296–305. [CrossRef]
38. Kingma, D.P.; Ba, J. Adam: A method for stochastic optimization. *arXiv* **2014**, arXiv:1412.6980.
39. Bekkar, M.; Djemaa, H.K.; Alitouche, T.A. Evaluation measures for models assessment over imbalanced data sets. *J. Inf. Eng. Appl.* **2013**, *3*, 27–38.
40. Pai, A. *Energy Function Analysis for Power System Stability*; Springer Science & Business Media: New York, NY, USA, 1989.
41. DIgSILENT GmbH. *Synchronous Machine TechRef ElmSym, TypSym*; DIgSILENT GmbH: Gomaringen, Germany, 2021.
42. Rudez, U.; Mihalic, R. WAMS-Based Underfrequency Load Shedding With Short-Term Frequency Prediction. *IEEE Trans. Power Deliv.* **2015**, *31*, 1912–1920. [CrossRef]
43. ABB. *Live Tank Circuit Breakers-Buyers Guide*, 4th ed.; ABB: Ludvika, Suecia, 2008.
44. Grassberger, P.; Schreiber, T.; Schaffrath, C. Nonlinear time sequence analysis. *Int. J. Bifurc. Chaos* **1991**, *1*, 521–547. [CrossRef]
45. van der Maaten, L.; Hinton, G. Visualizing data using t-SNE. *J. Mach. Learn. Res.* **2008**, *9*, 11.